Progress In Electromagnetics Research M, Vol. 57, 45–53, 2017

An Echo Simulation Method for DBS Imaging that Considers Environmental Factors

Gaosheng Li[1, *], Gui Gao[1], Yang Bai[2], Dongming Zhou[1], Wei Liu[1], and Jianghua Cheng[1]

Abstract—DBS (Doppler Beam Sharpening) imaging for scene matching terminal guidance is investigated. An echo simulation method for DBS of missile-borne radar that considers environmental factors is presented. The transmission signals of missile-borne radar are studied first. Next, the method for the modeling of the echo signals is discussed with consideration of environmental influences including the objects on the ground, radome and seasonal variations, especially undulation of the ground. The status of the surface of the earth as well as internal elements of the radar will influence the precision of the height measurement, thereby indirectly influencing the image matching. Undulating terrain can also cause changes in the electromagnetic characteristics that lie in the translation of image points; in addition, there is a close relationship between the position offset and the altitude of the image area. The operation flow of DBS is provided together with the method of generating reference images. Finally, an optical image of an airport and the simulation results using echoes are presented for validation.

1. INTRODUCTION

The scene matching guidance method is a key technique of precise guidance [1]. In addition, the technique of DBS is widely used in the imaging of missile-borne and air-borne radar as DBS is an efficient method for imaging the ground at high resolution [2]. The simulation of DBS to improve attack achievements has become a popular topic for investigation [3].

Missile-borne radar can use impulse linear frequency modulation signals with wide ranges of time and frequency to improve the precision of height measurement as well as the cross-range resolution [4]. To support a precise attack, the reference image of the target area must be prepared for the scene matching terminal guidance system [5]. The reference images are typically obtained by a scouting airplane or satellite before a war, and the data may be multi-spectral or from the digital elevation model (DEM) or the Synthetic Aperture Radar (SAR) [6]. Due to the variation of the operational mechanism and the data processing style of the scouting radar, together with the differences in terrain of the ground, environment of the area, etc., the real-time images are different from the obtained data [7]. To perform a simulation of the environment based on the scouted data and to generate reference images is of great importance [8].

Terminal guidance of image matching determines the current location by comparing real-time images obtained from the radar with images stored in the missile-borne computers and then modifies the flying route [9]. The vegetation will show regular variation as the seasons change, thereby influencing the real-time imaging of the seeker and thus negatively affecting the guidance [10]. Moreover, the terrain undulation changes the electromagnetic scattering characters [11], thus influencing the precision of height measurement of the missile as well as the resolution of imaging [12].

Received 21 March 2017, Accepted 15 May 2017, Scheduled 22 May 2017

* Corresponding author: Gaosheng Li (Gaosheng7070@vip.163.com).

[1] College of Electronic Science and Engineering, National University of Defense Technology, Changsha 410073, China. [2] College of Equipment Management and Safety Engineering, Air Force Engineering University, Xi'an 710051, China.

The transmission signals of the missile-borne radar and the echoes will be analyzed first, followed by the model of the environment; finally, the flow of DBS imaging and an example for validation are presented.

2. THE TRANSMISSION SIGNALS OF THE RADAR

The missile-borne radar uses linear frequency modulation (LFM) signals to improve the range resolution under the condition of the allowed average power. The carrier is $A_1 \cos(\omega_0 t + \phi_0)$. The LFM signal can be expressed as

$$s_i(t) = A_2 \text{rect}\left(\frac{t}{\tau}\right) \cos\left(\omega_0 t + \frac{\mu t^2}{2}\right) \tag{1}$$

where $\text{rect}(x)$ is the rectangular function

$$\text{rect}(x) = \begin{cases} 1 & |x| \le 1/2 \\ 0 & |x| > 1/2 \end{cases} \tag{2}$$

The envelope of the LFM signal is a rectangular pulse with a width of τ, whose transient angular frequency ω_i changes linearly with time.

$$\omega_i = d\phi/dt = \omega_0 + \mu t \tag{3}$$

The variation range of the angular frequency of the signal within the pulse width τ is $[2\pi f_0 - \frac{\mu\tau}{2}, 2\pi f_0 + \frac{\mu\tau}{2}]$, and the bandwidth of frequency modulation B is $\mu\tau/(2\pi)$.

The output of the LFM pulse after the frequency up-conversion by the carrier is

$$\begin{aligned} s_t(t) &= \sum_{n=0}^{\infty} p(t - nT) \\ p(t) &= \text{Arect}\left(\frac{t}{\tau}\right) \cos\left[\left((\omega + \omega_0)t + \phi_0 + \frac{\mu t^2}{2}\right)\right] \quad |t| \le \frac{\tau}{2} \end{aligned} \tag{4}$$

This result is merely the transmission signal of the missile-borne radar.

3. THE ECHO SIMULATION OF THE IMAGING

3.1. General Consideration of DBS

The speed vector can be treated as a constant in a quite short time span, and the assumption that the radar transmits and receives the pulse at the same location can meet the precision requirement of modeling of the echo. The operation situation of the height measurement antenna together with the imaging antenna is shown in Fig. 1. A sketch map of the illumination of the beam is given in Fig. 2.

Figure 3 indicates the coordinate for the simulation of the radar imaging, and Fig. 4 shows the focus of the beam of the wave when the platform flying.

Suppose that the azimuth pattern function of the antenna is $f(R, \theta)$ and that the reflection coefficient of the area illuminated by the wave is $f_\sigma(R, \theta)$. Furthermore, the space transferring factor is $L(R, \theta)$. In this case, the echo signals received by the radar can be indicated as

$$\tilde{s}_r(t) = \iint \frac{1}{R^2} \tilde{s}_t\left(t - \frac{2R}{c}\right) \cdot f_\sigma(R, \theta) f^2(R, \theta) L^2(R, \theta) \cdot r' dr' d\theta \quad \left|t - \frac{2R}{c}\right| \le \frac{\tau}{2} \tag{5}$$

where $\widetilde{S_r}$ and $\widetilde{S_t}$ denote the complex forms of the echo S_r and the transmission signal S_t, respectively. R is a function of r' and θ, i.e., $R(r', \theta)$, and $r'dr'd\theta$ is the tiny surface element of the illumination area. Here, r' stands for the measured distance with a small system error before calibration, which could usually meet the requirement for the certain precision. Based on the formula $R^2 = r'^2 + H^2$, we have $r'dr' = RdR$. Neglecting the gain factor of the radar system and considering the procedure of the down-conversion, the relative signal detection and I/Q detection as well as the sampling, and supposing

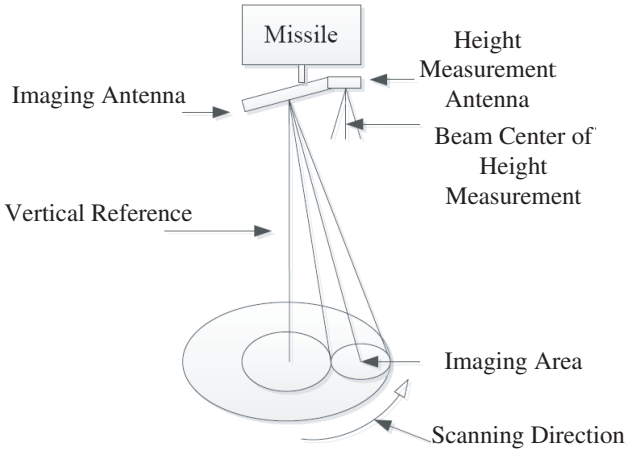

Figure 1. The operational situation of the antennas.

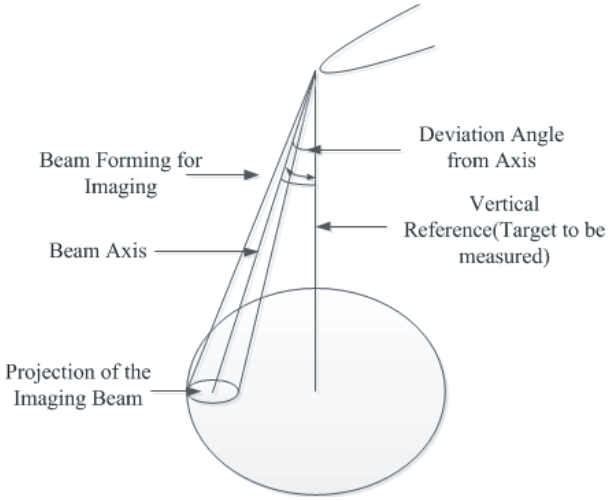

Figure 2. The illumination of the beam.

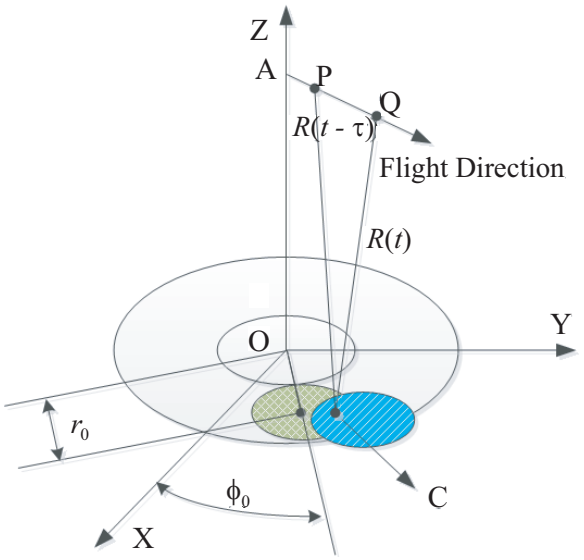

Figure 3. The imaging coordinate.

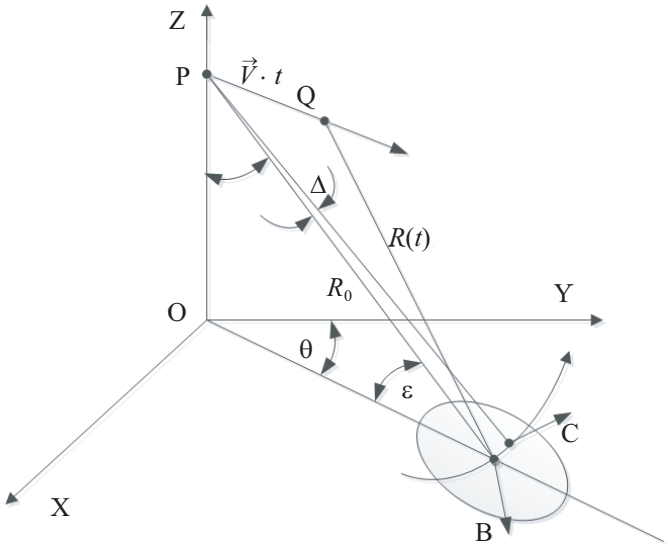

Figure 4. The focus of the beam of the wave when the platform flying.

that the distance of the adjacent sampling gate is ΔR, the output complex signals of I and Q detectors corresponding to each range gate are

$$\tilde{s}_{rIQ}(t) = \sum_{m=0}^{M-1} \int_{\theta}^{|F(R_m,\theta)|} \cdot \exp\left\{ j\left[\frac{4\pi}{\lambda} R_m(t) + \varphi(R_m,\theta) \right] \right\} \cdot R_m \Delta R d\theta \tag{6}$$

$$F(R_m,\theta) = \frac{1}{R^2} \left| f_\sigma(R,\theta) f^2(R,\theta) L^2(R,\theta) \right| e^{j\varphi(R_m,\theta)} \tag{7}$$

$$\varphi(R_m,\theta) = \varphi_{f_\sigma}(R_m,\theta) + \varphi_{f^2}(R_m,\theta) + \varphi_{L^2}(R_m,\theta) \tag{8}$$

where M is the number of the range gates and $\Delta R = c\tau_0/2$ (τ_0 is the pulse width after the compression).

Further discussion is required for the DBS imaging. A sampling data matrix with the order of

$N \times M$ can be obtained if we take N pulses in each patch processing period of the DBS imaging.

$$\tilde{s}_{rIQ}\left(t_{n,m}\right) = \int_{\theta_{1n}}^{\theta_{2n}} \left|F\left(R_m, \theta\right)\right| \cdot \exp\left\{j\left[\frac{4\pi}{\lambda} R_m\left(t\right) + \varphi\left(R_m, \theta\right)\right]\right\} \cdot R_m \Delta R d\theta \tag{9}$$

where $t_{n,m} = nT_r + m\tau_0, (n = 0, 1, \ldots, N-1; m = 0, 1, \ldots, M-1)$, $\theta_{1n} = \theta_0 - (\beta_{3\,\mathrm{dB}} + \Omega T)/2 + nT_r\Omega$, and $\theta_{2n} = \theta_{1n} + \beta_{3\,\mathrm{dB}}$.

The symbol Ω denotes the scanning angular speed of the antenna, and θ_0 is the central azimuth angle of the illumination area in a certain processing period. The term $F(R_m, \theta)$ in the formula consists of three items, namely, the influence of the antenna, the objects on the ground and the space environment.

3.2. The Environmental Factors in the Modeling of the Echo Signals

Different objects on the ground have different scattering characteristics. Suppose the complex dielectric coefficient of the ground surface is $\tilde{\varepsilon}_r = \varepsilon'_r + j\varepsilon''_r$, and the incidence angle of the wave corresponding to the surface unit is Δ. The complex reflection coefficients for the polarization of vertical and horizontal becomes

$$\begin{aligned} \Gamma_v &= \frac{\tilde{\varepsilon}_r \cos\Delta - \sqrt{\tilde{\varepsilon}_r - \sin^2\Delta}}{\tilde{\varepsilon}_r \cos\Delta + \sqrt{\tilde{\varepsilon}_r - \sin^2\Delta}} \\ \Gamma_h &= \frac{\cos\Delta - \sqrt{\tilde{\varepsilon}_r - \sin^2\Delta}}{\cos\Delta + \sqrt{\tilde{\varepsilon}_r - \sin^2\Delta}} \end{aligned} \tag{10}$$

In fact, the backward scattering feature will be random to some extent because of the undulation of the ground and numerous interferences, diffractions and reflections.

Set the backward scattering coefficient to be $\sigma^0(\alpha)$. The incidence angle is determined by the given DEM data, the beam parameters of the missile-borne antenna and the ballistic conditions. The extent of the coarse surface that the ground spot represented by the pixel point in the source image as well as the backward scattering coefficient corresponding to the incidence angle α_0 can be obtained from the database of the materials.

The scattering factor of the ground object $f_\sigma(R_m, \theta)$ has a relationship with $\sigma^0(\alpha)$.

$$\sigma^0\left(\alpha\right) = E\left[\left|f_\sigma\left(R_m, \theta\right)\right|^2\right] \tag{11}$$

where $E[\cdot]$ denotes the average value of the surface resolution unit on the ground.

Due to the variation of the objects on the ground as well as the environment, it is difficult to express the backward reflection coefficients by an accurate formula or a uniform method. The database containing the features of the objects on the ground must be built to meet the requirement of the simulation under various circumstances.

High frequency approaching algorithms can be applied to the target with the size of several times of the resolution unit. To find the contribution points first and then determine the diffracted coefficients, the scattering field can be obtained.

Generally, the main lobe of the azimuth pattern function of the antenna is fairly flat, especially the phase that can be treated as a constant. However, the pattern of amplitude and phase may be aberrated due to the burning of the radome when the missile returns the atmosphere. The algorithm of plane wave-ray tracking can be used to compute the performance of the integration of the antenna and the radome.

Real-time radar images are obtained from low-altitude (usually several kilometers) aircraft. To eliminate the influence of short distance compression on the inclined direction image, the horizontal distance imaging mode is used. The geometric forms of the real-time image and the reference image are concordant when the dominant factor that would influence the matching is the difference between their radiation features. When there exists height undulation, the figure building modes would be differentiated adequately to influence the precision of the matching and guidance.

To realize guidance with high precision, the characteristics of the scattering features according to the vegetation in spring, summer, autumn and winter must be studied. A database is required to be built in typical areas to support precise attack. Because crops such as wheat, rice and sugarcane will

show clear differences during their lifespans, agricultural areas would reflect different signals on the radar. For some grasslands, the water content is high in the summer whereas for others it is lower in winter, even withering or leaving the soil naked.

The features of the materials that combine the objects on the ground have important influences on the radar echoes, which is mainly determined by the complex dielectric constant. Generally, the higher the complex dielectric constant becomes, the stronger that it reflects the radar waves and the shorter distance that the radar waves can penetrate into the material. Table 1 indicates the changes in the echo amplitudes of grasslands in band Ka with the season alternance.

Table 1. Changes in the echo amplitudes of grasslands with the season alternance at band Ka.

Month	3	4	5	6	7	8	9	10
Echo (dB)	−17.5	−15.5	−11	−10	−10.5	−11.5	−12	−12.5

3.3. The Influence of the Ground Undulation

SAR imaging is a type of range imaging. When there is undulation on the ground, the pixel shift in the direction of range will be

$$dy = -h\cos\theta/r \tag{12}$$

where h is the height difference of the reference plane, and r is the pixel resolution.

When the amplitude of undulation of the ground is relatively high (more than 50 m), accurate imaging formulas must be established and geometric calibration must be performed. It is better to consider the DEM (Digital Elevation Model) data to eliminate the image distortion caused by the terrain undulation.

The terrain undulation will directly result in a change of calculation of the inclined range. The echo signal of the undulation point will correspond to the point in the horizontal point of the same inclined range that causes the geometric change of the image, as shown in Fig. 5.

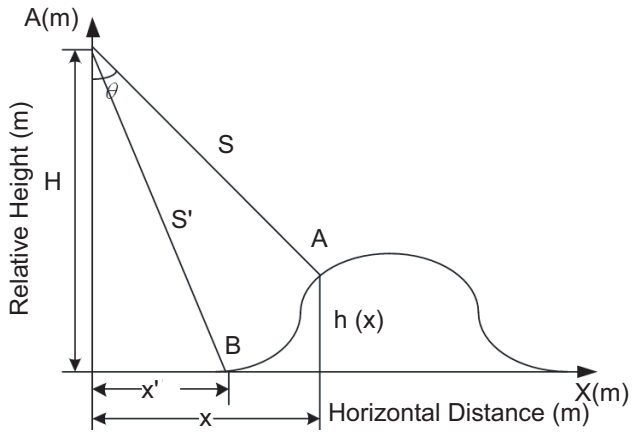

Figure 5. Sketch of the terrain undulation.

To study the influence of terrain undulation on the image matching performance of the radar, we set the height variation to follow the 2-D Gauss distribution function

$$f(x,y) = \frac{1}{\sqrt{2\pi}\sigma} e^{-\frac{(x-\mu)^2+(y-\mu)^2}{2\sigma^2}} \tag{13}$$

where μ is the mean value, σ^2 the variance, and $f(x,y)$ the height. To choose the typical values for $(\mu,\sigma) = (300,150)$, (1200, 600), and (2600, 1300), the relative $f(x,y)$ represents plain, hill and mountain.

Suppose the size of the radar image is fixed, and the sampling rate changes with the imaging height H according to certain proportion. The image resolution is $R = H/r$. The deviation amount of the imaging point

$$\Delta x_1 = \Delta x/R \tag{14}$$

$$K = x/H = tg\theta \tag{15}$$

$$p = h(x)/H \tag{16}$$

The calibration based on the vertical projection is

$$x' = \sqrt{(H - h(x))^2 + x^2 - H^2} = H\sqrt{K^2 - (2p - p^2)} \tag{17}$$

The deviation amount of the resolution element in the real time image relative to the reference image is

$$\Delta x = x - x' = H\left(K - \sqrt{K^2 - (2p - p^2)}\right) \tag{18}$$

It could be further transformed into

$$\Delta x = r\left(K - \sqrt{K^2 - (2p - p^2)}\right) = \frac{r(2p - p^2)}{K + \sqrt{K^2 - (2p - p^2)}} \tag{19}$$

A set of typical values are as follows:

$r = H/R$, $H = 4,000\,\mathrm{m}$, $R = 5\,\mathrm{m}$, $K = x/H$, $p = h(x)/H = f(x,y)/H$. where $f(x,y)$ is the above-mentioned Gauss distribution function.

Thus, the influence of the terrain undulation on the imaging can be deduced as the translation of image points. The follow-up processing can be conducted on the image to obtain the distortion figures and then complete the image matching.

It can be found from the above-described formula that the deviation of image points is related to the imaging height and the extent of terrain undulation. The ratio of the amplitude of undulation of the ground to the imaging height usually satisfies the condition of $p < 0.5$; thus, if H increases, then p will decrease, and the deviation of the image point Δx_1 will also decrease. If the amplitude of undulation of the ground $h(x)$ increases, then p and the deviation of the image point will increase as well.

3.4. The Calculations and the Results

The missile performs a straight line flight in a short-time span, and the main radiation beam of the antenna is needle-like. The illuminated area is divided into small fan-shaped resolution elements. Suppose the reflection coefficient of the ground of each resolution element is

$$f(R,\theta) = |f(R,\theta)| \exp\{j\phi(R,\theta)\} \tag{20}$$

The reflection echoes of each resolution element are proportional to the following:

$$A(\theta)|f(R,\theta)| \cos\left[\omega\left(t - \frac{2R(t)}{C}\right) - \phi(R,\theta)\right] RdRd\theta \tag{21}$$

Take the symbol $r(t)$ to represent the echo of the whole area illuminated by the radar radio beam.

$$r(t) = \int_R \int_\theta A(\theta)|f(R,\theta)| \cos\left[\omega\left(t - \frac{2R(t)}{C}\right) - \phi(R,\theta)\right] RdRd\theta \tag{22}$$

where $A(\theta)$ is the azimuth pattern function of the antenna, $2R(t)/C$ the time delay of the reflection echoes, $RdRd\theta$ the area of the resolution unit, and R the slanting distance. The echoes are received by the radar and then conducted to the mixer and the intermediate frequency (IF) amplifier. The IF signal will be transferred into the orthogonal coherent detector, whose output would be complex signals of the form:

$$r(t) = \int_R \int_\theta |f(R,\theta)| \exp\left\{j\left[\frac{4\pi}{\lambda} \cdot R(t) + \phi(R,\theta)\right]\right\} RdRd\theta \tag{23}$$

The imaging procedures of DBS are as follows and as shown in Fig. 6.

i. To sample the echoes first;

ii. To store the echo data of different times in a matrix by sequence, and the data of the same range gate will be located in the same line;

iii. To pre-filter the N echoes of the same range gate and different time to avoid the effect of overlapping;

iv. To perform FFT for the N echoes to obtain the imaging data of the same beam and range but different azimuth;

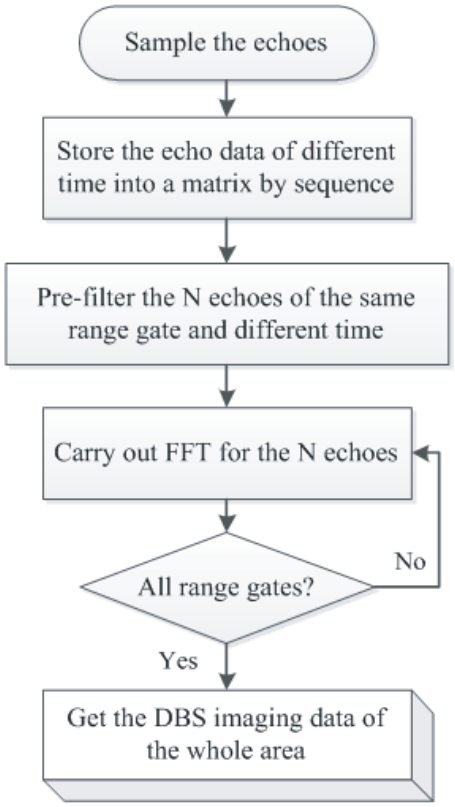

Figure 6. The imaging procedures of DBS.

Figure 7. An optical image of a certain airport.

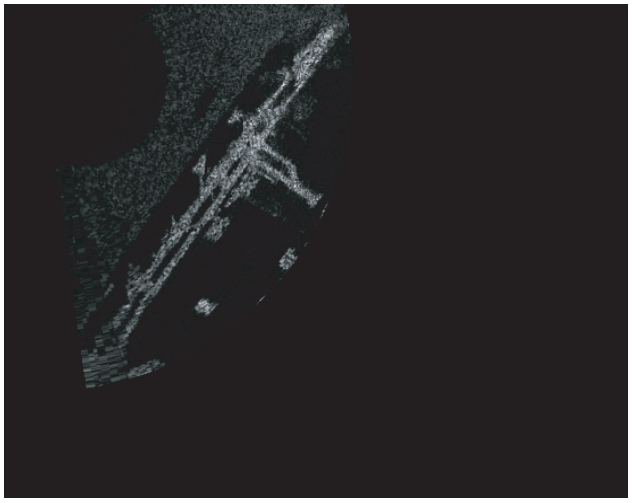

Figure 8. The DBS image based on echo simulations.

v. Repeat the operation of Step iv for echoes of different range gates to obtain the DBS imaging data of the whole area.

The optical image of a certain airport is given in Fig. 7. The DBS image based on echo simulations is shown in Fig. 8.

It can be observed from Fig. 7 and Fig. 8 that the height of the missile is 6.6 km, the speed vector $(55\overrightarrow{x} + 302\overrightarrow{y} - 1054\overrightarrow{z})m/s$, the impulse width 6 µs, the compression ratio 120, the pulse repeating frequency (PRF) 5 kHz, the width in azimuth of the antenna pattern 24° and that in range 3.8°, and the scanning speeding 360 degrees/s. The weather is sunny, without snow or water on the ground.

4. CONCLUSION

The changes in ground vegetation introduced by the alternating change of season together with the height change of the terrain undulation influence the real-time imaging of guided missiles. The primary form of the influence is the amplitude decrease by attenuation and the signal distortion by scattering. The situation of the ground surface and the internal technical indexes of the radar are disadvantageous to the scene matching. Furthermore, many other factors, such as the matching algorithms, condition of the weather, flying speed, features of the radome and error of angle measurement, influence the matching and guidance performance and thus require investigation and compensation to ensure a precise attack.

Obtaining reference images for a scene matching terminal guidance system of missiles using the method of echo simulation is possible after building a database of scattering features of ground objects with consideration of environmental influences.

REFERENCES

1. Liu, F., F. Zhao, Y. Deng, W. Yu, and J. Ai, "A new high resolution DBS imaging algorithm based on least squares linear fitting," *Journal of Electronics and Information Technology*, Vol. 33, No. 4, 787–791, 2011.
2. Choi, S., J. Chun, I. Paek, and K. Yoo, "A new approach of FMCW-DBS altimeters for terrain-aided navigation," *4th Asia-Pacific Conference on Synthetic Aperture Radar*, 214–217, Tsukuba, Japan, Sep. 2013.
3. Chen, H., M. Li, Y. Lu, and Y. Wu, "DBS image stitching algorithm based on affine transformation," *IET International Radar Conference*, Xi'an, China, Apr. 2013.
4. Qiao, H. and J. Zhang, "Research on cruise missile alarm and defense system," *Radio Engineering*, Vol. 39, No. 2, 24–27, 2009.
5. Kang, X., G. Cheng, Y. Qiao, and S. Chen, "A terminal guidance law design applied to space-to-surface precision attack weapon," *Journal of Solid Rocket Technology*, Vol. 32, No. 2, 11–14, 2009.
6. Ye, Q. and Y. Cheng, "Impact of Terrain undulation on precision of radar scene matching," *Journal of Remote Sensing*, Vol. 9, No. 1, 106–111, 2005.
7. Yang, W., T. Zhang, X. Wang, and N. Sang, "Analysis of the hypsography influence on the positioning performance of radar scene matching," *Infrared and Laser Engineering*, Vol. 32, No. 3, 304–308, 2003.
8. Wang, H., Z. Zhao, Y. Cai, and W. Fang, "An efficient method improving the suitability of scene matching guidance images," *Guidance and Fuze*, Vol. 25, No. 4, 7–11, 2004.
9. Sang, N., X. Lu, and Z. Zuo, "The application of digital elevation information to radar scene matching," *Journal of Huazhong University of Science and Technology*, Vol. 32, No. 4, 102–104, 2004.
10. Chen, H., M. Li, Z. Wang, Y. Lu, S. Wang, L. Zuo, P. Zhang, and Y. Wu, "Super-resolution Doppler beam sharpening imaging via sparse representation," *IET Radar, Sonar & Navigation*, Vol. 10, No. 3, 442–448, 2016.

11. Sorokin, A. K. and Y. G. Vazhenin, "Linear references detection by pulse altimeter with Doppler beam sharpening," *IEEE 4th Asia-Pacific Conference on Antennas and Propagation*, 556–557, Bali Island, Indonesia, Jun. 2015.
12. Zhou, X., Y. Huang, W. Li, Z. Li, and J. Yang, "DBS Doppler centroid estimation based on mutual information maximization," *IET International Radar Conference*, Hangzhou, China, Oct. 2015.